Performance Analysis of Vectored Wireline Systems Embracing Channel Uncertainty

Thomas Magesacher[1], Driton Statovci[2], Tomas Nordström[2,3] and Erwin Riegler[4]
[1]Department of Electrical and Information Technology, Lund University, Box 118, SE-22100 Lund, Sweden
[2]FTW Forschungszentrum Telekommunikation Wien GmbH, Donau-City-Strasse 1, A-1220 Vienna, Austria
[3]Centre for Research on Embedded Systems (CERES), Halmstad University, Box 823, SE-30118 Halmstad, Sweden
[4]Institute of Telecommunications, Vienna University of Technology, Gusshausstrasse 25, A-1040 Vienna, Austria
Email: tom@eit.lth.se, {statovci, nordstrom}@ftw.at, tomas.nordstrom@hh.se, erwin.riegler@tuwien.ac.at

***Abstract*—Future wireline communication systems aspire to boost the throughput in two ways: First, they exploit higher frequencies to gain more bandwidth on shorter lines in combination with vectoring. Second, they use non-differential transmission modes (such as phantom modes, common modes, split-pair modes) to exploit more dimensions. Performance predictions for systems exploiting these techniques are of great importance for upgrading copper networks to provide Internet access or deploying copper-based backhaul systems to connect mobile base-stations. Good predictions require accurate channel models. However, channel modeling for higher frequencies and non-differential modes is still in its infancy. A mixed deterministic/stochastic channel model is proposed to remedy this problem. The outage rate is derived based on an asymptotic (in the number of participating transceivers) analysis. As application examples, performance predictions in access networks using phantom modes and frequencies up to 200 MHz are presented.**

I. Introduction

Broadband Internet access via the in-place copper network is an important part of today's fixed broadband-access infrastructure [1] and will likely continue to play a key role in the evolutionary development process of future broadband access systems [2]. Recently mobile-network operators began to investigate the possibility of exploiting the existing copper infrastructure to provide backhaul connectivity in small-cell networks.

Co-location of transceivers on one side allows for coordination of transceivers with the aim of better exploiting the potential of the cable through techniques summarized under the term dynamic spectrum management (DSM) [3]. The level of coordination ranges from single-line power control (DSM level 1) over multi-line spectrum control (DSM level 2) to joint signal processing (DSM level 3). Cooperation of transmitters or receivers on signal-level at the last distribution point can be modeled as a broadcast channel or a multiple access channel, respectively. Corresponding pre-coding and interference cancellation techniques are often summarized under the term vectoring or vectored transmission [4]–[8]. Network operators have used DSM level 1 and level 2 to improve the performance and stability of their systems. Recently they have started deploying vectored systems (DSM level 3) mainly from street cabinets aiming at increasing data rates [9].

Emerging wireline communication systems boost the achievable rate mostly in two ways. First, they use higher frequencies on short lines [2], [10]. Second, they employ alternative transmission modes (phantom modes, common modes, split-pair modes) [11]–[14]. Performance prediction for such systems is a major challenge since the development of reliable models for high-frequency behavior and non-differential modes is ongoing and the verification in real networks is time-consuming [11], [15]–[18]. At the same time, such predictions and models can be of great practical value since they influence operators' investment decisions.

In this work, the problem is approached by modeling parts of the channel as a mixture of a deterministic and a stochastic component. Wireline channels are frequency selective and vary very slowly over time. The concept of outage probability and outage rate is applied to capture variations of wireline channel properties from line to line in a network.

The paper is organized as follows. Section II presents the system and channel model. Section III derives the outage rate. Section IV presents application examples and Section V concludes the work.

II. System and Channel Model

We consider the setup depicted in Figure 1. There are $N+1$ modem pairs (x_i, y_i), $i = 0, \ldots, N$ which are connected via direct paths (wire-pairs in a cable) and crosstalk paths (crosstalk-coupling paths). Paths starting from x_0 and paths terminating in y_0 are modeled as a sum of a deterministic and a stochastic coefficient (dashed red lines). All remaining paths (solid blue lines) are assumed to be known perfectly[1].

The received signals $\mathbf{y} = \begin{bmatrix} y_0 & y_1 & \cdots & y_N \end{bmatrix}^{\mathrm{T}} \in \mathbb{C}^{N+1}$ are processed jointly and we are interested in the performance of the link $(x_0, \mathbf{y})$. Let $\mathbf{H} = \begin{bmatrix} \mathbf{h} & \mathbf{H}_I \end{bmatrix} \in \mathbb{C}^{(N+1)\times(N+1)}$ denote the channel matrix, where $\mathbf{h}$ is its first column and $\mathbf{H}_I$

This work was partly supported by: The Swedish Research Council (VR) through grant No. 621-2007-6309 and the Swedish Foundation for Strategic Research (SSF) through grant No. ICA08-0022. The WWTF grant ICT10-066. The Competence Center FTW Forschungszentrum Telekommunikation Wien GmbH is funded within the program COMET - Competence Centers for Excellent Technologies by BMVIT, BMWFJ, and the City of Vienna. The COMET program is managed by the FFG.

[1]The model can easily be extended so that more (or all) paths are mixed-deterministic/stochastic.

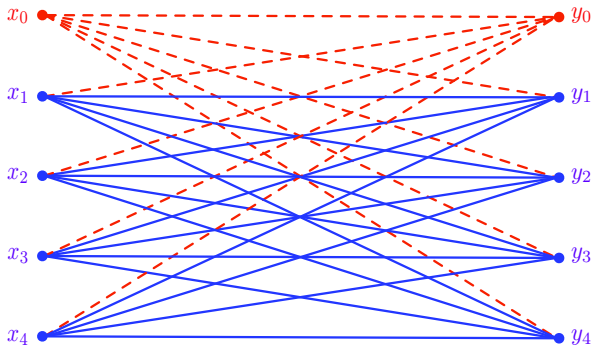

Fig. 1. Mixed deterministic/stochastic channel model ($N = 4$).

contains the remaining columns. The received signal vector $\mathbf{y}$ can be written as

$$\mathbf{y} = \mathbf{h}x_0 + \mathbf{H}_I\mathbf{x}_I + \mathbf{z}. \tag{1}$$

Here, the complex jointly-Gaussian circularly symmetric random vector $\mathbf{z} \sim \mathcal{CN}(\mathbf{0}, \mathbf{N})$ with covariance matrix $\mathbf{N}$ models noise. The transmitted signal x_0 and the interfering signal vector $\mathbf{x}_I = \begin{bmatrix} x_1 & x_2 & \dots & x_N \end{bmatrix}^{\mathrm{T}}$ are assumed to be Gaussian distributed, *i.e.*, $x_0 \sim \mathcal{CN}(0, P_0)$, where P_0 denotes the variance of x_0 and $\mathbf{x}_I \sim \mathcal{CN}(\mathbf{0}_N, \mathbf{P}_I)$ with $\mathbf{P}_I \triangleq \mathrm{diag}(P_1, P_2, \dots, P_N)$.

Let $\bar{\mathbf{H}} = \begin{bmatrix} \bar{\mathbf{h}} & \bar{\mathbf{H}}_I \end{bmatrix}$ denote the deterministic part of the channel matrix, where $\bar{\mathbf{h}}$ is the first column and $\bar{\mathbf{H}}_I$ contains the remaining columns. The channel is modeled according to

$$\begin{cases} \mathbf{h} & \triangleq \bar{\mathbf{h}} + \mathbf{R}^{1/2}\mathbf{w} \in \mathbb{C}^{(N+1)\times 1} \\ \mathbf{H}_I & \triangleq \bar{\mathbf{H}}_I + \mathbf{R}_I^{1/2}\mathbf{W}_I\mathbf{T}_I^{1/2} \in \mathbb{C}^{(N+1)\times N} \end{cases} \tag{2}$$

where $\mathbf{w} \in \mathbb{C}^{(N+1)\times 1}$ and $\mathbf{W}_I \in \mathbb{C}^{(N+1)\times N}$ have zero mean complex Gaussian independent and identically distributed entries with variance one. The matrices $\mathbf{R} \triangleq \mathrm{diag}(\sigma_0, \sigma_1, \dots, \sigma_N)$ and $\mathbf{T}_I \triangleq \mathrm{diag}(\rho_1, \rho_2, \dots, \rho_N)$ contain the variances of the stochastic parts of the channel matrices. More specifically, σ_i is the variance of the stochastic part of path (x_0, y_i) and ρ_i is the variance of the stochastic part of path (x_i, y_0). The matrix $\mathbf{R}_I \triangleq \mathrm{diag}(1, \mathbf{0}_N)$ acts as a projection and takes into account that only the interfering links from x_i, $i \in \{1, 2, \dots, N\}$ to y_0 contain stochastic components.

The model described by (2) applies to each subcarrier of a discrete multi-tone wireline communication system. The paths (x_n, y_n) model the direct channels and the paths $(x_m, y_n), m \neq n$ model far-end crosstalk (FEXT).

III. Outage Analysis

Since real and imaginary parts of the channel coefficients are modeled as Gaussian random variables with non-zero mean, the channel coefficients' magnitudes have a Rician distribution. In order to quantify the uncertainty of individual channel coefficients we define the Rician factors

$$\mathrm{K}_{m,n} \triangleq |[\bar{\mathbf{H}}]_{m,n}|^2 / (\mathbb{E}[|[\mathbf{H}]_{m,n}|^2] - |[\bar{\mathbf{H}}]_{m,n}|^2). \tag{3}$$

The Rician factor is the quotient between "direct" and "diffuse" received signal power.

Under the assumption that the receiver knows exactly the realizations of the channel matrix $\mathbf{H} = \begin{bmatrix} \mathbf{h} & \mathbf{H}_I \end{bmatrix}$, the random mutual information is given by [19]

$$\begin{aligned} I \triangleq \ln\det(\mathbf{I}_{N+1} + P\mathbf{h}\mathbf{h}^H + \mathbf{H}_I\mathbf{P}_I\mathbf{H}_I^H) \\ - \ln\det(\mathbf{I}_{N+1} + \mathbf{H}_I\mathbf{P}_I\mathbf{H}_I^H) \end{aligned} \tag{4}$$

expressed in nat per complex dimension. In order to calculate the asymptotic (in terms of N) cumulant moments of I, which are needed to derive the outage probability, we reformulate a result in [19, Theorem 1], which allows to calculate the asymptotic mean μ_I and variance σ_I^2 of I. Furthermore, [19, Theorem 1] states that all higher moments of I tend to zero as $N \to \infty$, so that I converges in distribution to the Gaussian random variable $\mathcal{N}(\mu_I, \sigma_I^2)$. The derivation of the asymptotic outage probability follows, *mutatis mutandis*, the derivation in [20] and yields

$$p(I) = \frac{1}{\sqrt{2\pi\sigma_I^2}} \exp\left(-\frac{(I-\mu_I)^2}{2\sigma_I^2}\right).$$

Hence, for a fixed power P, we find for the maximum rate I_ϵ such that $\Pr(I < I_\epsilon) < \epsilon$

$$I_\epsilon = \mu_I - \sigma_I Q^{-1}(\epsilon), \tag{5}$$

where $Q(x) \triangleq 1/(2\pi)\int_x^\infty \exp(-u^2/2)\mathrm{d}u$.

IV. Applications

This section demonstrates the application of the mixed deterministic/stochastic channel model (2) and the concept of outage analysis to investigate the impact of channel modeling uncertainty in vectoring scenarios. The throughput results presented hereinafter include a signal-to-noise-ratio (SNR) gap of 12.9 dB corresponding to a coding gain of 3 dB, an SNR margin of 6 dB, and a target symbol error rate for quadrature amplitude modulation of 10^{-7}. With an SNR gap Γ, the throughput R_ϵ and the corresponding bound R are given by $R_\epsilon = \log_2(1 + (2^{I_\epsilon} - 1)/\Gamma)$ and $R = \log_2(1 + (2^{\mu_I} - 1)/\Gamma)$, respectively.

A. Example 1

In many networks, customers are connected via two pairs to the last distribution point allowing for the use of two differential modes (x_1, y_1), (x_2, y_2) and a phantom mode (x_0, y_0) [11]—a classic example illustrated in Figure 2. A number of issues have to be considered when exploiting alternative modes such as the phantom mode. For example, phantom modes are more susceptible to ingress[2] and are likely to cause more egress. Furthermore, the background noise encountered on phantom modes in the field might be higher than the commonly used differential-mode level of -140 dBm/Hz. Modeling alternative transmission modes is more involved than modeling differential modes and usually requires a larger

[2]In wireline communications, ingress and egress are referred to as electromagnetic radiation picked up and radiated by wires, respectively.

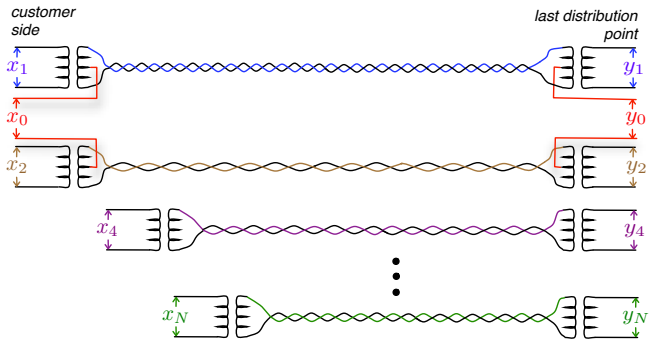

Fig. 2. Example 1. Phantom-mode transmission over two pairs. Two twisted wire pairs can accommodate two differential modes (x_1, y_1) and (x_2, y_2) and one phantom mode (x_0, y_0). $N = 8$.

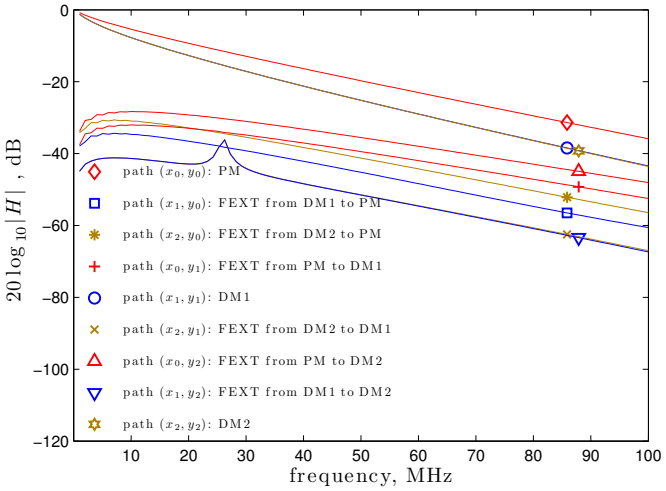

Fig. 3. Example 1. Magnitude responses of direct and far-end crosstalk (FEXT) paths in a 200 m 2-pair wireline system with three modes: two differential modes (DM) and one phantom mode (PM).

number of parameters [11], [15]–[18]. Even if a line in the network can be characterized perfectly, parameters vary over lines in the network. The goal of this example is to demonstrate how to tackle the difficulty of modeling phantom modes and related crosstalk paths by capturing channel uncertainties with the mixed deterministic/stochastic model (2).

Figure 3 depicts the magnitude responses of a 200m 2-pair channel generated using multi-conductor transmission line theory [15], [16] (wire diameter: 0.5 mm; conductor material: copper; insulation thickness 0.36 mm; insulation material: polyethylene; twist-lengths: 0.05 m and 0.155 m). In comparison to phantom modes, differential paths can be modeled fairly accurately. For simplicity, we assume perfect knowledge of all differential-mode related direct and crosstalk paths while the lack of accurate phantom-mode models is taken into account by

$$\mathrm{K}_{m,n} = \begin{cases} K & \text{for } m = 0, n = 0, \ldots, 2 \\ K & \text{for } m = 0, \ldots, 2,\ n = 0 \\ \infty & \text{otherwise} \end{cases}.$$

For illustration, Figure 4 shows the relation between Rician factor and channel-magnitude deviation from the mean for 99% ($\epsilon = 10^{-2}$) and 99.9999% ($\epsilon = 10^{-6}$) of the channels.

For the numerical throughput results presented in the following, a frequency range of 1–100 MHz is considered and the frequency-flat transmit and noise power spectral densities (PSDs) are -75 dBm/Hz and -130 dBm/Hz, respectively. Figure 5 shows the achievable rates on the three modes using vectoring. Note that the throughput results assume that the vectoring systems in the network can learn the actual channel coefficients perfectly—the goal of the analysis is to capture the variation of phantom-mode channel properties over lines. The results for $\epsilon = 10^{-2}$ and $\epsilon = 10^{-6}$ can be interpreted as achievable rates supported by 99% and 99.9999% of the channels encountered in the field for the channel uncertainty factor K, respectively.

The phantom mode supports a higher rate than the differential mode since it uses both pairs which increases the effective wire diameter. Each differential mode supports a

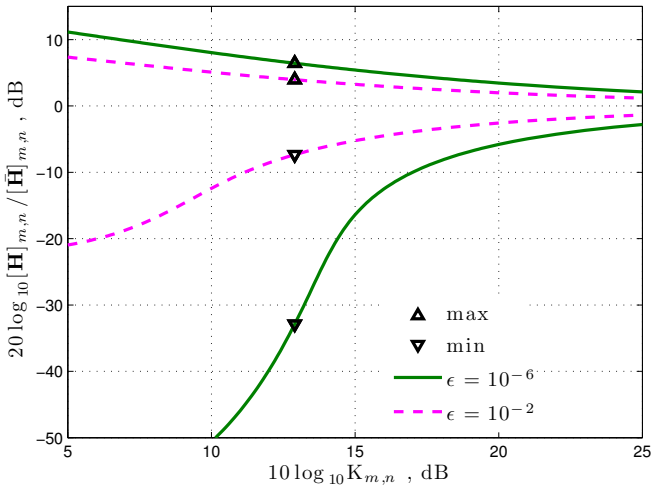

Fig. 4. Channel uncertainty versus Rician factor $\mathrm{K}_{m,n}$: with probability $1-\epsilon$ the channel coefficient's magnitude deviation is within the bounds. Solid lines: $\epsilon = 10^{-6}$. Dashed lines: $\epsilon = 10^{-2}$.

rate of about 254 Mbit/s. Assume we want to achieve three times that rate, *i.e.*, 762 Mbit/s, by using the two differential modes and one phantom mode in order to make phantom-mode transmission worthwhile. Based on the asymptotic analysis, we can conclude that phantom-mode transmission is worthwhile in the above sense when the channel uncertainty does not exceed a level corresponding to roughly $K = 7.2$ dB for $\epsilon = 10^{-2}$. For $\epsilon = 10^{-6}$, a lower channel uncertainty (corresponding to roughly $K = 13.1$ dB) is required to make phantom-mode transmission worthwhile in the above sense.

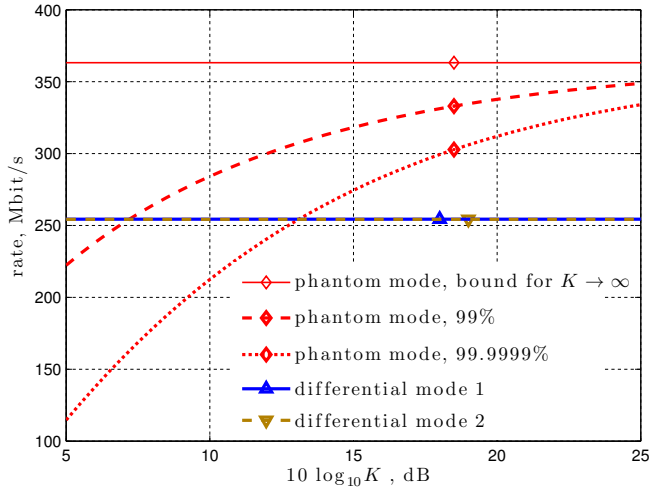

Fig. 5. Example 1. Achievable rate with an SNR gap of 12.9 dB versus Rician factor K.

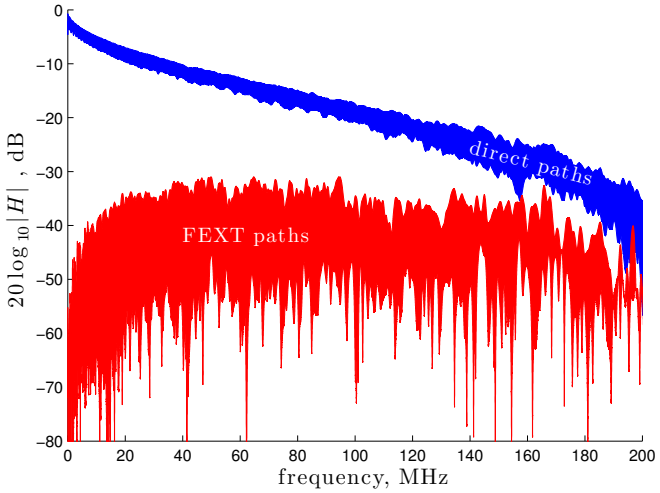

Fig. 6. Example 2. Measured spread of direct paths and FEXT paths in a 24-pair 0.5 mm-cable of 100 m length.

B. Example 2

For cables as short as a few hundred meters, the low direct-channel attenuation allows the use of frequencies beyond 100 MHz. Using higher bandwidth on shorter lines is the main approach to deliver rates in the order of Gbit/s to customer premises in the access network.

Despite recent progress such as the ITU-T standardization effort G.fast [21], which specifies a high-speed high-bandwidth time-division duplexed transmission scheme over short copper lines, network characterization beyond 30 MHz is still in its early stages. Even for frequencies below 30 MHz the variation of direct and crosstalk path coefficients from line to line in a cable can be substantial and even more so from cable to cable. For frequencies beyond 30 MHz, this variation is expected to grow. The concept of outage rate is used in order to capture this spread in performance predictions.

We consider a 24-pair 0.5 mm-cable of 100 m length. Figure 6 illustrates the magnitude spread of direct paths and FEXT paths based on measurements of 10 pairs (resulting in a frequency-dependent 10×10 channel coefficient matrix) of one cable segment in the frequency range 4 kHz–200 MHz.

Based on the measurement results, the deterministic parts of the channel coefficients and the Rician factors can be estimated. Figure 7 shows the frequency-dependent Rician factors for the direct path and for the FEXT path estimated from 10 and 90 measured coefficients per frequency point, respectively. While the Rician factors indicate a decreasing spread of FEXT-path magnitudes with increasing frequency, there is a trend towards larger spreads for higher frequencies in direct paths—an observation confirmed by a number of measurement campaigns [21]. The spread of path-magnitudes within a cable is considerable and it is reasonable to expect even larger spreads over same-type cables in the network.

We now consider a scenario with 10 vectored lines ($N = 9$) and assume that all paths consist of deterministic and stochastic components with the Rician factors shown in Figure 7. The frequency-flat transmit and noise PSDs are -75 dBm/Hz and -140 dBm/Hz, respectively. Figure 8 shows the spectral efficiency in bit/s/Hz for link $(x_0, \mathbf{y})$ versus frequency as well as the gap in spectral efficiency with respect to the bound obtained when all Rician factors approach infinity. For 99% of the channels, the spectral-efficiency gap with respect to the mean channel does not exceed 2 bit/s/Hz. For 99.9999% of the channels, the spectral-efficiency gap with respect to the mean channel is not larger than roughly 3 bit/s/Hz. The results for the other links $(x_i, \mathbf{y})$, $i = 1, \ldots, 9$ are very similar since all pairs have the same length.

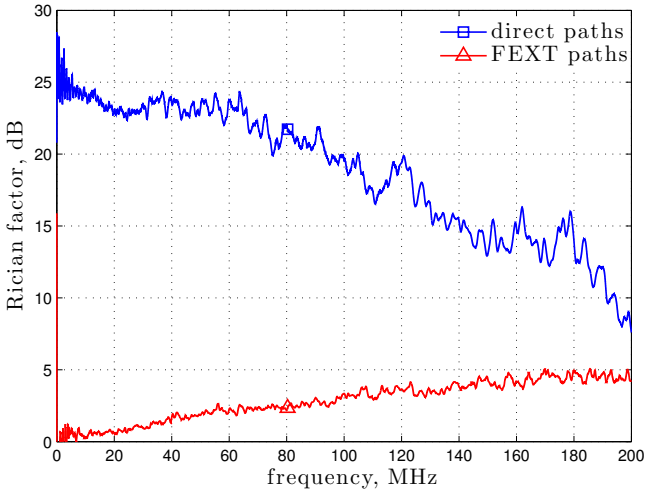

Fig. 7. Example 2. Rician factors estimated from measurements shown in Figure 6.

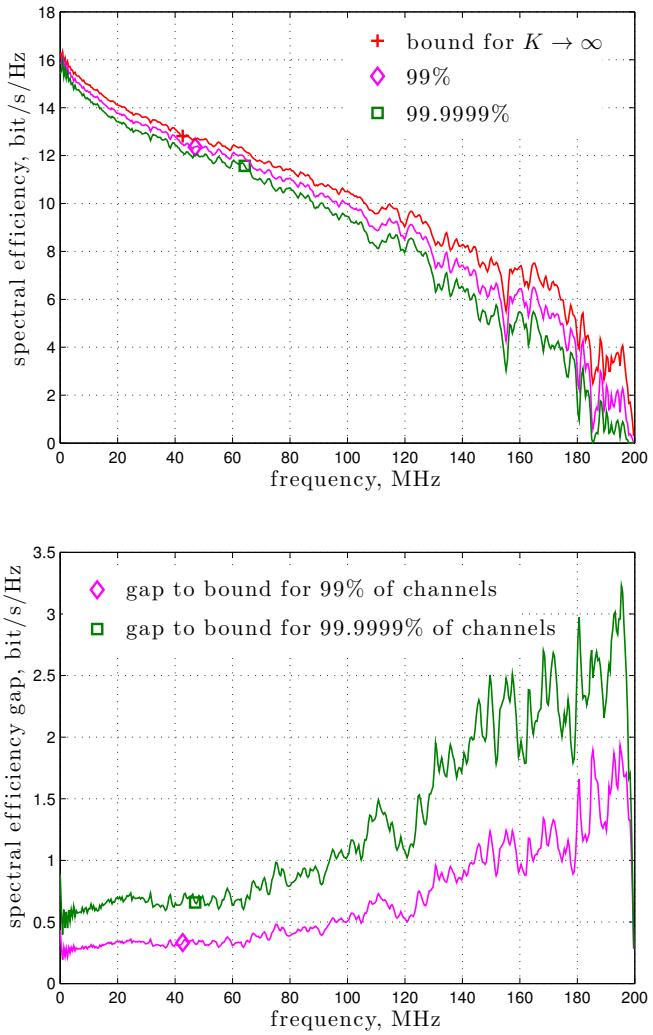

Fig. 8. Example 2. Top: Spectral efficiency with an SNR gap of 12.9 dB (diamond marker: $\epsilon = 10^{-2}$. square marker: $\epsilon = 10^{-6}$) for the Rician factors shown in Figure 7 versus frequency and corresponding bound (plus marker). Bottom: Spectral efficiency gap with respect to bound.

V. Conclusion

Channel uncertainty is a situation frequently encountered when analyzing future wireline communications. The outage analysis for vectoring scenarios is a useful remedy to allow performance predictions for such situations.

Typical application examples are performance prediction in access networks using alternative transmission modes and/or bandwidths beyond 100 MHz. The sheer lack of reliable channel models complicates such forecasts. Outage-rate analysis can provide a basis for infrastructure decisions although only partial knowledge of the network's copper-channel properties is available.

References

[1] V. Oksman, H. Schenk, A. Clausen, J. M. Cioffi, M. Mohseni, G. Ginis, C. Nuzman, J. Maes, M. Peeters, K. Fisher, and P.-E. Eriksson, "The ITU-T's new G.vector standard proliferates 100 Mb/s DSL," *IEEE Communications Magazine*, vol. 48, no. 10, pp. 140–148, Oct. 2010.

[2] P. Ödling, T. Magesacher, S. Höst, P. O. Börjesson, M. Berg, and E. Areizaga, "The fourth generation broadband concept," *IEEE Communications Magazine*, vol. 47, no. 1, pp. 62–69, Jan. 2009.

[3] K. B. Song, S. T. Chung, G. Ginis, and J. M. Cioffi, "Dynamic spectrum management for next-generation DSL systems," *IEEE Communications Magazine*, vol. 40, no. 10, pp. 101–109, Oct. 2002.

[4] G. Ginis and J. M. Cioffi, "Vectored transmission for digital subscriber line systems," *IEEE Journal on Selected Areas in Communications*, vol. 20, no. 5, pp. 1085–1104, Jun. 2002.

[5] R. Cendrillon, M. Moonen, J. Verlinden, T. Bostoen, and G. Ginis, "Improved linear crosstalk precompensation for DSL," in *Proc. IEEE International Conference on Acoustics, Speech, and Signal Processing (ICASSP), 2004*, vol. 4, Montreal, Quebec, Canada, May 2004, pp. 1053–1056.

[6] R. Cendrillon, M. Moonen, E. Van den Bogaert, and G. Ginis, "The linear zero-forcing crosstalk canceler is near-optimal in DSL channels," in *Proc. IEEE Global Telecommunications Conference (GLOBECOM), 2004*, vol. 4, Dallas, Texas, USA, Nov–Dec 2004, pp. 2334–2338.

[7] R. Cendrillon, M. Moonen, G. Ginis, K. Van Acker, T. Bostoen, and P. Vandaele, "Partial crosstalk cancellation for upstream VDSL," *EURASIP J. Appl. Signal Process.*, vol. 2004, no. 10, pp. 1520–1535, Jan. 2004. [Online]. Available: http://dx.doi.org/10.1155/S1110865704309273

[8] R. Cendrillon, G. Ginis, M. Moonen, and K. Van Acker, "Partial crosstalk precompensation in downstream VDSL," *Signal Process.*, vol. 84, no. 11, pp. 2005–2019, Nov. 2004. [Online]. Available: http://dx.doi.org/10.1016/j.sigpro.2004.07.013

[9] ITU, *Very high speed digital subscriber line transceivers 2 (VDSL2), Technical Recommendation G.993.2*, ITU Std., Dec. 2011.

[10] T. Magesacher, J. Rius i Riu, P. Ödling, P. O. Börjesson, M. Tilocca, and M. Valentini, "Limits of ultra-wideband communication over copper," in *Proc. International Conference on Communication Technology (ICCT) 2006*, Guilin, China, Nov. 2006, pp. 1–4.

[11] W. Foubert, C. Neus, L. Van Biesen, and Y. Rolain, "Exploiting the phantom-mode signal in DSL applications," *IEEE Transactions on Instrumentation and Measurement*, vol. 61, no. 4, pp. 896–902, Apr. 2012.

[12] T. Magesacher, P. Ödling, P. O. Börjesson, W. Henkel, T. Nordström, R. Zukunft, and S. Haar, "On the capacity of the copper cable channel using the common mode," in *Proc. IEEE Global Telecommunications Conference (GLOBECOM) 2002*, vol. 2, Taipei, Taiwan, Nov. 2002, pp. 1269–1273.

[13] J. M. Cioffi, S. Jagannathan, M. Mohseni, and G. Ginis, "CuPON: the copper alternative to PON 100 Gb/s DSL networks," *IEEE Communications Magazine*, vol. 45, no. 6, pp. 132–139, Jun. 2007.

[14] S. Jagannathan, V. Pourahmad, K. Seong, J. M. Cioffi, M. Ouzzif, and R. Tarafi, "Common-mode data transmission using the binder sheath in digital subscriber lines," *IEEE Transactions on Communications*, vol. 57, no. 3, pp. 831–840, Mar. 2009.

[15] C. R. Paul, *Analysis of Multiconductor Transmission Lines*. ISBN 0-471-02080-X, Wiley, 1994.

[16] T. Magesacher, "MTL—A multi-wire transmission line modeling toolbox," *International Journal of Computer and Electrical Engineering*, vol. 5, no. 1, pp. 52–55, Feb. 2013.

[17] B. Lee, J. M. Cioffi, S. Jagannathan, K. Seong, Y. Kim, M. Mohseni, and M. Brady, "Binder MIMO channels," *IEEE Transactions on Communications*, vol. 55, no. 8, pp. 1617–1628, Aug. 2007.

[18] M. Jakovljevic, T. Magesacher, K. Ericson, P. Ödling, P. O. Börjesson, and S. Zazo, "Common mode characterization and channel model verification for shielded twisted pair (STP) cable," in *Proc. IEEE International Conference on Communications (ICC) 2008*, Beijing, China, May 2008, pp. 447–451.

[19] E. Riegler and G. Taricco, "Asymptotic statistics of the mutual information for spatially correlated Rician fading MIMO channels with interference," *IEEE Transactions on Information Theory*, vol. 56, no. 4, pp. 1542–1559, Apr. 2010.

[20] D. Tse and P. Viswanath, *Fundamentals of wireless communication*. New York, NY, USA: ISBN 0-5218-4527-0, Cambridge University Press, 2005.

[21] R. F. M. van den Brink (TNO), "G.fast: Wideband transfer and crosstalk measurements on twisted pair cables," *ITU-T-SG15 contribution 11BM-021 to "G.fast"*, Apr. 2011.